

The evolution of localized Gaussian vortices in planar homogenous shear flows

M. Karp and J. Cohen

*Faculty of Aerospace engineering, Technion - Israel Institute of Technology,
Haifa 32000, Israel*

I. Shukhman

*Institute of Solar-Terrestrial Physics, Russian Academy of Sciences,
Siberian Department, Irkutsk 664033, P.O. Box 291, Russia*

Wall bounded and free turbulent shear flows have been observed to contain organized coherent structures such as hairpin vortices, counter-rotating vortex pairs (CVP's) and streaks (regions of high and low velocity). In order to be able to follow the temporal evolution of such coherent structures we have developed an analytical based method which is capable of following the evolution of a localized disturbance in flows with constant homogenous shear, in which the base velocity varies at most linearly with space. In this paper we briefly present the method and some preliminary results characterizing the development of localized Gaussian vortices, having various initial amplitudes and orientations, embedded in different types of base flows.

I. Introduction

Coherent vortical structures observed in turbulent boundary layer have been reported by [1] as early as 1967. In this pioneering work two kinds of coherent structures have been identified: (i) counter-rotating vortex pairs (CVP's), which lead to the creation of streaks (regions of high and low velocity), and (ii) hairpin (or horseshoe) vortices, which consist of a pair of streamwise vortices connected by a short spanwise 'head' segment. It has been found that the hairpin vortices are inclined at approximately 45° relative to the base flow. Since then, a growing list of researchers have reported the existence of the aforementioned coherent structures in a variety of wall-bounded turbulent and transitional shear flows. The appearance of these structures under various flow conditions suggests that these structures play a key role in self-sustained turbulence and various transition scenarios.

In recent years, a simple model describing the evolution of the aforementioned coherent structures has been developed. The model follows the evolution of a localized disturbance (in space). The main assumption of the model is that the disturbance is localized and therefore "sees" only the homogenous shear surrounding it, i.e, the velocity of the surrounding base flow varies at most linearly with space. The model was originally employed by [2] to calculate the interaction between a localized vortical disturbance and

pure shear (Couette) flow. Calculations were performed using the software FLUENT. Afterwards, the model was extended using a novel, analytical-based method, to include any homogenous shear flow, using the software MATLAB. The focus of this paper is to present the analytical-based method and demonstrate its applications to various flows. The mathematical method is first discussed in the next section, followed by results associated with various base flows and disturbance initial conditions, and main conclusions.

II. Mathematical Method

The analytical-based method is described thoroughly in Cohen *et al.* [3]. Without loss of generality the base-flow velocity and vorticity are given by

$$\mathbf{V} = \left(-\frac{1}{2}(\Omega + \sigma)y, -\frac{1}{2}(\sigma - \Omega)x, 0\right), \quad \boldsymbol{\Omega} = (0, 0, \Omega), \quad (1)$$

where σ and Ω are two constants representing the shear and vorticity of the base flow. The equation describing the evolution of vorticity ($\boldsymbol{\omega}$) associated with a 3D finite-amplitude localized disturbance in incompressible viscous base flow is

$$\frac{\partial \boldsymbol{\omega}}{\partial t} + (\mathbf{V} \cdot \nabla) \boldsymbol{\omega} - (\boldsymbol{\omega} \cdot \nabla) \mathbf{V} - (\boldsymbol{\Omega} \cdot \nabla) \mathbf{v} = \nu \Delta \boldsymbol{\omega} + (\boldsymbol{\omega} \cdot \nabla) \mathbf{v} - (\mathbf{v} \cdot \nabla) \boldsymbol{\omega}, \quad (2)$$

where t is time, ν the kinematic viscosity and the disturbance vorticity $\boldsymbol{\omega}$ and velocity \mathbf{v} are related by $\boldsymbol{\omega} = \nabla \times \mathbf{v}$.

By performing a transformation from real space (\mathbf{r}) to Fourier space (\mathbf{k}), using lagrangian variables (\mathbf{q}) and designating

$$\boldsymbol{\zeta}(\mathbf{q}, t) = \hat{\boldsymbol{\omega}}(\mathbf{k}(\mathbf{q}, t), t), \quad (3)$$

where $\hat{\boldsymbol{\omega}}(\mathbf{k})$ is the Fourier transform of the vorticity and $\boldsymbol{\zeta}(\mathbf{q})$ is the Fourier transform in lagrangian variables, we are able to obtain a convenient form of the equations for the evolution of the vortical disturbance

$$\frac{d\zeta_1(\mathbf{q}, t)}{dt} = -\frac{1}{2}(\sigma - \Omega) \zeta_2(\mathbf{q}, t) - \Omega k^{-2} k_1 \left[k_1 \zeta_2(\mathbf{q}, t) - k_2 \zeta_1(\mathbf{q}, t) \right] - \nu k^2 \zeta_1(\mathbf{q}, t) + \hat{N}_1(\mathbf{q}, t), \quad (4a)$$

$$\frac{d\zeta_2(\mathbf{q}, t)}{dt} = -\frac{1}{2}(\sigma + \Omega) \zeta_1(\mathbf{q}, t) - \Omega k^{-2} k_2 \left[k_1 \zeta_2(\mathbf{q}, t) - k_2 \zeta_1(\mathbf{q}, t) \right] - \nu k^2 \zeta_2(\mathbf{q}, t) + \hat{N}_2(\mathbf{q}, t), \quad (4b)$$

$$\frac{d\zeta_3(\mathbf{q}, t)}{dt} = \Omega k^{-2} k_3 \left[k_1 \zeta_2(\mathbf{q}, t) - k_2 \zeta_1(\mathbf{q}, t) \right] - \nu k^2 \zeta_3(\mathbf{q}, t) + \hat{N}_3(\mathbf{q}, t). \quad (4c)$$

These equations are easily integrated in time (in Fourier space) and then the vorticity in real space is calculated applying the inverse Fourier transform. Various integration methods have been tested and Euler's method (first order) was found to be sufficient and used to obtain the following results.

III. Results

A. Model verification

The initial Gaussian disturbance is given by

$$\boldsymbol{\omega}(\mathbf{r}, t = 0) = \nabla F \times \mathbf{P}_0, \quad F = (\pi^{1/2}\delta)^{-3} \exp(-r^2/\delta^2), \quad (5)$$

where r is the spherical radial coordinate, δ is the representative length scale of the disturbance and \mathbf{P}_0 is its initial fluid impulse. The initial orientation of the vortex, ϕ , is the angle between \mathbf{P}_0 and the positive x axis. The strength of the initial vortex is characterized by $\varepsilon = \omega_{\max}(t = 0)/\Omega_*$, where $\omega_{\max}(t = 0) = 0.154|\mathbf{P}_0|/\delta^4$ and $\Omega_* = \frac{1}{2}(|\Omega| + |\sigma|)$. The magnitude of ε is used to describe an initial vortex as linear ($\varepsilon \ll 1$) or non linear. Length scales are normalized by δ and time scales are normalized by $1/\Omega_*$. The disturbance Reynolds number is $Re = \Omega_*\delta^2/\nu$.

The model was verified with analytical results obtained for the linear case [4, 5, 6, 7] and DNS simulations performed by the software FLUENT for pure shear (unbounded Couette, $\Omega = \sigma$) flow [2] and for plane stagnation (irrotational, $\Omega = 0$) flow [8]. A comparison of the obtained structure from DNS is shown in figure 1. The reader is referred to [3] for quantitative verification (e.g, vorticity distributions) of the method.

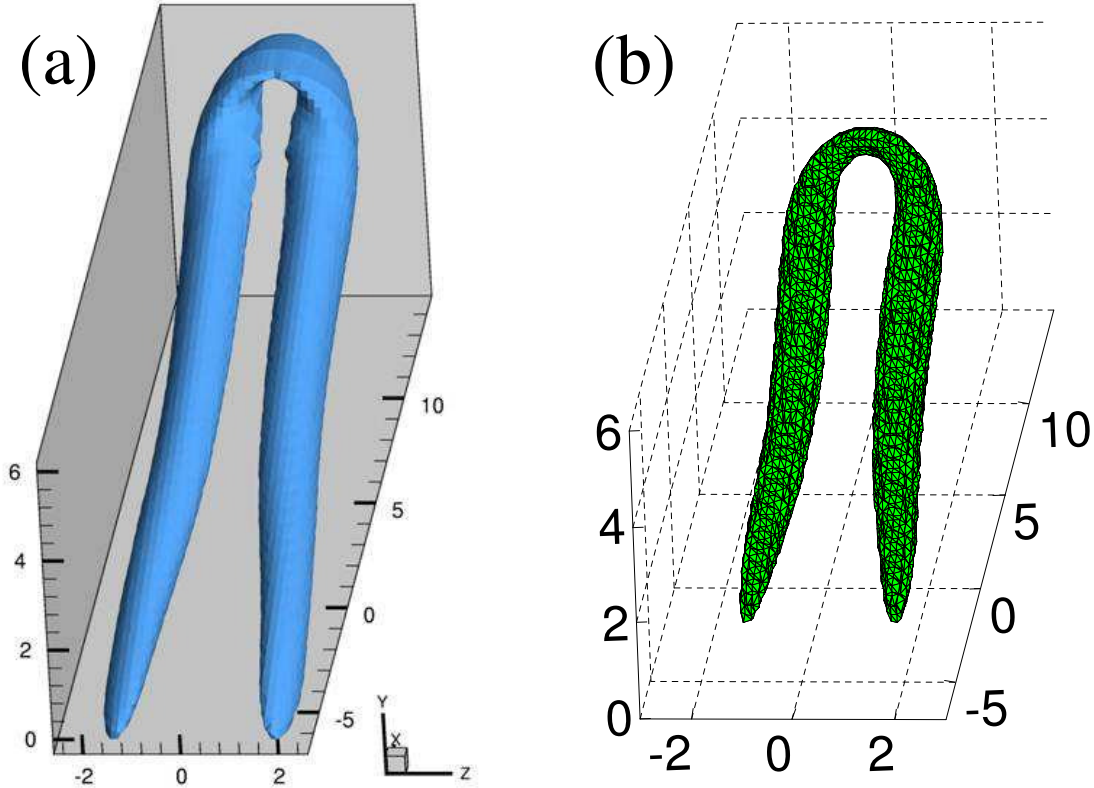


Figure 1. Single hairpin evolved from an initial Gaussian vortex. The structure at $T = 5$ is shown by $0.5Q_{max}$ iso-surface of Q definition, obtained by (a) DNS [2]; (b) the current method

B. Vortex identification

In addition to vorticity magnitude iso-surface plots (e.g. $0.7\omega_{max}$ iso-surface), we plot iso-surfaces of Q definition (e.g figure 1). Q definition is the second invariant of the velocity gradient tensor $\nabla\mathbf{v}$. It is defined by

$$Q = -\frac{1}{2}u_{i,j}u_{j,i} \quad (6)$$

where $u_{i,j} = \partial u_i / \partial x_j$ and repeating indices imply the usual summation convention.

Additional characteristics are integral quantities, such as the vortex strength, its center and inclination angle [2]. The strength of the vortical disturbance, W , is measured by the volume integral of the enstrophy, $\|\boldsymbol{\omega}\|^2$. Therefore, it is also referred as the total enstrophy. The center of the vortical structure (CVS) is the first moment of the enstrophy, normalized by the vortex strength (this definition is analogous to center of gravity). The vortex inclination angle, α , has been introduced in [5] and describes the angle between the vortex elongation axis and the x axis. For a disturbance, which is symmetric with respect to the $z = 0$ plane (which is the focus of this work), the expression for α is

$$\alpha = \frac{1}{2} \arctan \left(\frac{2T_{12}}{T_{11} - T_{22}} \right) + \frac{1}{4}\pi(1 + s) - \frac{1}{2}\pi, \quad s = \text{sign}(T_{11} - T_{22}). \quad (7)$$

where T_{ij} is the tensor of enstrophy distribution (the reader is referred to [5] for additional information).

C. Parameters

A parametric investigation of the following parameters has been performed: (a) base flow parameters, σ and Ω . The parameters were chosen to maintain a constant value of $\Omega_* = 40[1/s]$. The parameter $\lambda = (\sigma - \Omega)/(\sigma + \Omega)$ is used to identify the base flow. The base flow is referred as hyperbolic for $|\sigma| > |\Omega|$, elliptic for $|\sigma| < |\Omega|$ and pure shear for $|\sigma| = |\Omega|$. The limiting case for hyperbolic flow is irrotational flow with $\Omega = 0, \lambda = 1$ and the one for elliptic flow is pure rotational flow with $\sigma = 0, \lambda = -1$. The following set of values was examined $\lambda = -1 : 0.25 : 1$; (b) vortex initial orientation, with the following set of values: $\phi = 0^\circ : 10^\circ : 180^\circ$; (c) initial amplitude of the vortex, $\varepsilon = 0.015, 1, 7.5$ for linear, weakly non linear (WNL) and highly non linear (HNL) cases respectively;

The simulations were performed for $\delta = 10^{-3}[m]$ and $\nu = 10^{-6}[m^2/s]$. These parameters together with $\Omega_* = 40[1/s]$ maintain $Re = 40$ for all the cases.

D. Parametric investigation

First, we present an example of the obtained structures. A Gaussian disturbance with initial orientation of $\phi = 90^\circ$ can be seen in figure 2a. For the case of irrotational flow ($\Omega = 0$) and linear disturbance ($\varepsilon \ll 1$) a CVP is obtained, the structure can be seen in figure 2b. For the case of Couette flow ($\Omega = \sigma$) and non linear ($\varepsilon = 7.5$) disturbance a hairpin is obtained, the structure can be seen in figure 2c.

The total enstrophy, normalized by its initial value, as a function of time and initial vortex orientation is shown in figure 3 for various base flows. The total enstrophy for the linear and WNL cases is very similar. Thus, only the WNL and HNL cases are presented.

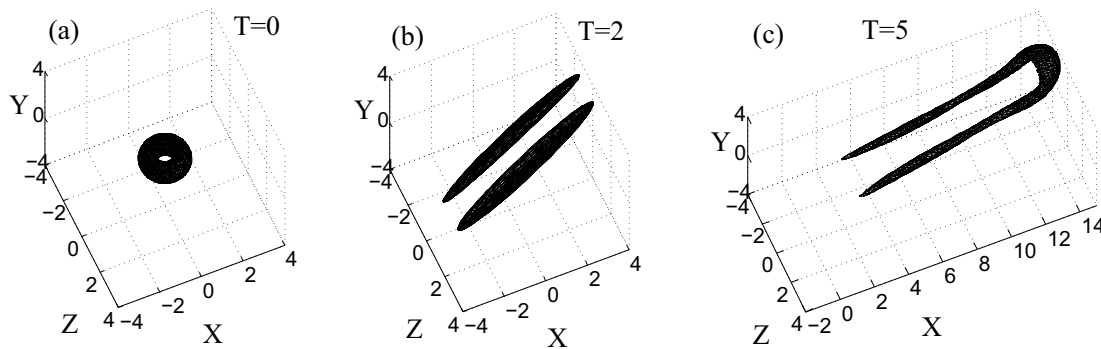


Figure 2. (a) the initial Gaussian disturbance (b) VCP obtained for irrotational flow, linear case (c) hairpin obtained for Couette flow, non linear case

As can be seen in figure 3, the hyperbolic flow attains the maximal growth. Moreover, the disturbance grows more rapidly for the hyperbolic case (note that the different time scale for the hyperbolic flow). For the pure shear and hyperbolic flows there is a wide range of initial orientations ($70^\circ < \phi < 180^\circ$) for which the disturbance grows, whereas a disturbance embedded in the elliptic flow grows initially for those orientations but eventually decays at long times. The optimal orientation is in the range $120^\circ < \phi < 140^\circ$ for the hyperbolic flow and $110^\circ < \phi < 130^\circ$ for pure shear. In all of the above, the growth for the HNL disturbance is larger, however qualitatively similar to the WNL (and linear) case.

The strength of a vortex, initially aligned with the x axis ($\phi = 90^\circ$), as a function of time is shown for various base flows in figure 4 for WNL and HNL disturbances. It can be seen that there is a correlation between λ and the growth rate. The amplification rate is the largest for the irrotational flow, $\lambda = 1$, whereas the attenuation rate is the largest for the pure rotating flow, $\lambda = -1$. For all hyperbolic flows the vortex grows at all times before exiting the computational domain. For all elliptic flows the vortex decays before achieving a significant amplification. The main differences between the WNL (and linear) and HNL cases are observed at short times ($T < 2$) where some initial amplification in the HNL case is observed. This difference occurs due to non-linear self induced motion which is mostly dominant at short times.

The self induced motion is demonstrated in figure 5 which shows the CVS for the case of pure shear flow and disturbance initial orientations of $\phi = 0^\circ, 60^\circ, 120^\circ, 180^\circ$ having various initial amplitudes. The vortex is initially positioned at the origin and the time step between two consecutive symbols is $\Delta T = 0.25$. It can be seen that in the linear case the vortex stays in the origin. For the WNL case, the vortex initially moves slightly from its initial position, however, there is a very small (negligible) effect on the overall development of the vortex. In the HNL case, the vortex initially moves in the direction of its orientation, and then continues to progress due to self induced motion and convection by the base flow. The linear equations (without the non linear terms) are symmetric [6]. Therefore, an initially symmetric vortex remains symmetric throughout the entire evolution. Thus, non linearity is required to break the symmetry and allow the formation of hairpins.

The vortex angle for various initial orientations for the hyperbolic flow having $\lambda = 0.5$

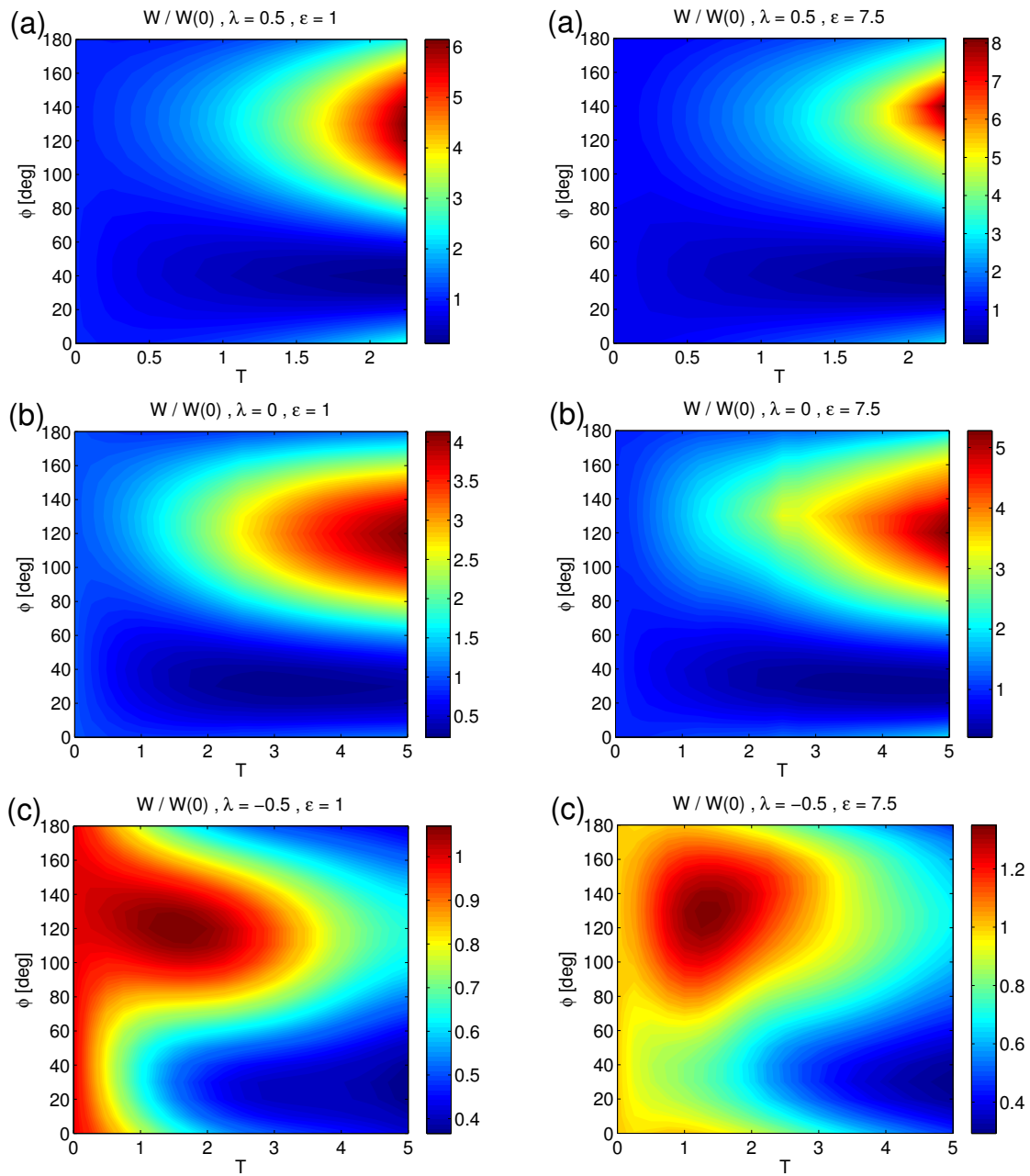


Figure 3. The total enstrophy vs. time and initial vortex orientation for (a) hyperbolic flow, $\lambda = 0.5$; (b) pure shear; (c) elliptic flow, $\lambda = -0.5$; WNL ($\varepsilon = 1$) on the left column and HNL ($\varepsilon = 7.5$) on the right column

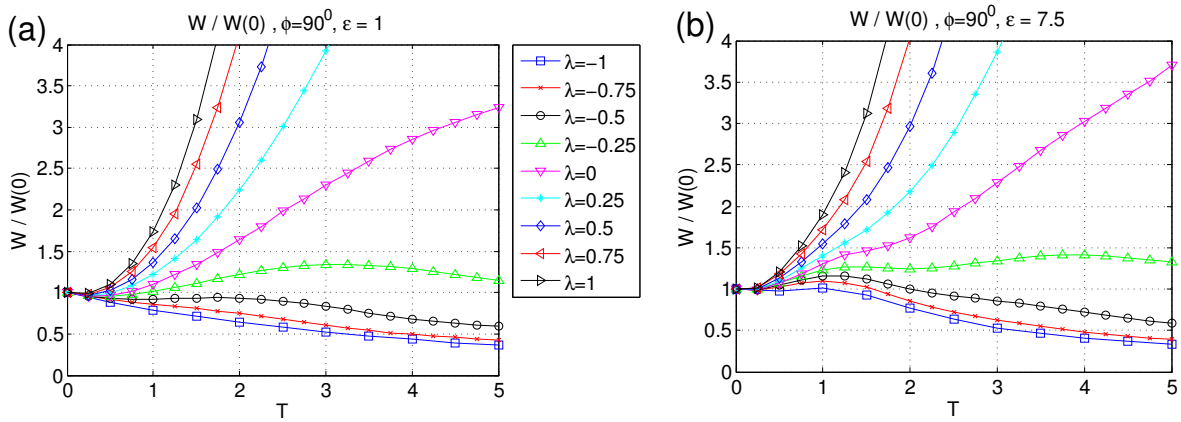


Figure 4. The total enstrophy vs. time for various base flows (λ) for (a) WNL; (b) HNL; initial vortex orientation of $\phi = 90^\circ$

can be seen in figure 6. The WNL and HNL cases are presented. Hyperbolic flows have two principal axes associated with strain extension and contraction, along which the velocity is directed outwards and inwards the origin, respectively. The angle of these asymptotes is given by $\tan \theta = \pm\sqrt{\lambda}$. The angle of the extensional asymptote is $\theta = \arctan(1/\sqrt{2}) \approx 35.3^\circ$ and it is indicated in figure 6 by the dashed line. It can be seen the vortex initially rotates to $35^\circ < \alpha < 45^\circ$ ($T = 1$) and then its final inclination angle slowly approaches the angle of the extensional asymptote (implying stretching of the vortex along the extensional axis). The initial rotation rate in the HNL case is almost twice faster than the initial rate associated with the WNL and linear cases. It can be seen that while there is a small scattering of the final angle for the WNL and linear cases, the scattering is more significant for the HNL case. The most amplified vortices ($120^\circ < \phi < 140^\circ$) are those having an initial angle close to the asymptote. Those vortices are preferred over the other vortices which ‘waste’ energy during the rotation process.

IV. Conclusions

An analytical based model capable of following the evolution of coherent structures in turbulent boundary layer flows has been developed. Analysis for various homogenous shear base flows has been performed. It has been found that there are negligible differences between linear ($\varepsilon = 0.015$) and WNL ($\varepsilon = 1$) cases, albeit the presence of non linear effects for the latter. Vortices embedded in hyperbolic flows have been found to grow while those embedded in elliptic flow decayed, even though in some cases they grew initially.

The model can be used for any localized disturbance and is also capable of following the evolution of non localized, periodic disturbances.

Acknowledgments

This research was supported by the Israeli Science Foundation (grant No. 1394/11) and Russian Science Support Foundation (RFBR grant No. 10-05-00094).

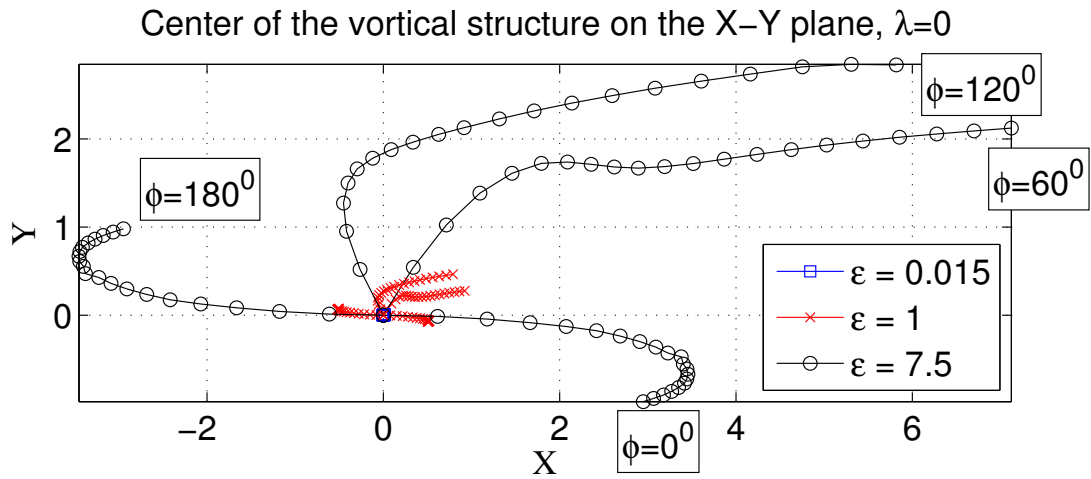


Figure 5. Vortex center on the X-Y plane for pure shear flow, for various orientations and initial amplitudes

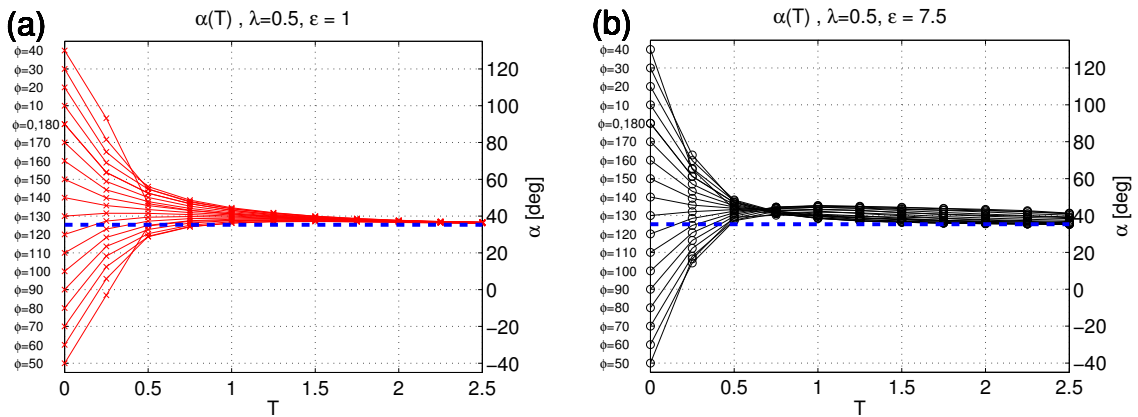


Figure 6. Vortex angle vs. time for various initial orientations for a hyperbolic base flow having $\lambda = 0.5$ (a) WNL; (b) HNL; the dashed line represents the extensional principal axis

References

1. Kline, S. J., Reynolds, W. C., Schraub, F. A., and Runstadler, P. W., “The structure of turbulent boundary layers,” *J. Fluid Mech.*, Vol. 30, 1967, pp. 741–773.
2. Saponitsky, V., Cohen, J., and Bar-Yoseph, P. Z., “The Generation of Streaks and Hairpin Vortices from a Localized Vortex Embedded in Unbounded Uniform Shear Flow,” *J Fluid Mech*, Vol. 535, 2005, pp. 65–100.
3. Cohen, J., Shukhman, I., Karp, M., and Philip, J., “An analytical-based method for studying the nonlinear evolution of localized vortices in planar homogenous shear flows,” *Journal of Computational Physics*, Vol. 229, 2010, pp. 7765–7773.
4. Shukhman, I. G., “Evolution of a localized vortex in plane nonparallel viscous flows with constant velocity shear: I. Hyperbolic flow,” *Phys. Fluids*, Vol. 18, 2006, pp. 097101.
5. Shukhman, I. and Levinski, V., “The evolution of the three-dimensional localized vortices in shear flows. Linear stage,” *Published online in arxiv.org/pdf/physics/0212101*, 2004.
6. Shukhman, I. and Levinski, V., “Evolution of the three-dimensional localized vortices in shear flows. Linear theory,” *Elektronnii Zhurnal Issledovano v Rossii (in Russian)*, 2003.
7. Shukhman, I. G., “Evolution of a localized vortex in plane nonparallel viscous flows with constant velocity shear: II. Elliptic flow,” *Phys. Fluids*, Vol. 19, 2007, pp. 017106.
8. Philip, J. and Cohen, J., “The Evolution of a Finite-Amplitude Localized Disturbance in an Irrotational Unbounded Plane Stagnation Flow,” *J. Fluid Mech.*, Vol. 555, 2006, pp. 459 – 473.